Sodium Thiosulfate acts as an H₂S mimetic to prevent intimal hyperplasia via inhibition of tubulin polymerization

Diane Macabrey[1,2], Alban Longchamp[1,2], Michael R. MacArthur[3], Martine Lambelet[1,2], Severine Urfer[1,2], Jean-Marc Corpataux[1,2], Sebastien Deglise[1,2*] and Florent Allagnat[1,2*]

[1] Department of Vascular Surgery, Lausanne University Hospital, Switzerland

[2] Department of Biomedical Sciences, University of Lausanne, Switzerland

[3] Department of Health Sciences and Technology, Swiss Federal Institute of Technology (ETH) Zurich, Zurich, Switzerland.

*These authors contributed equally to this work.

Corresponding Author :

Florent Allagnat

CHUV-Service de chirurgie vasculaire

Département des Sciences Biomédicales

Bugnon 7A, 1005 Lausanne, Suisse

Florent.allagnat@chuv.ch

Short title: sodium thiosulfate inhibits intimal hyperplasia

Keywords: Intimal hyperplasia; smooth muscle cells; proliferation; hydrogen sulfide; sodium thiosulfate.

Category: Original article

Word count: 7679 words

Total number of figures and tables: 6

Abstract

Background

Intimal hyperplasia (IH) remains a major limitation in the long-term success of any type of revascularization. IH is due to vascular smooth muscle cell (VSMC) dedifferentiation, proliferation and migration. The gasotransmitter Hydrogen Sulfide (H_2S) inhibits IH in pre-clinical models. However, there is currently no clinically approved H_2S donor. Here we used sodium thiosulfate (STS), a clinically-approved source of sulfur, to limit IH.

Methods

Hypercholesterolemic LDLR deleted (LDLR$^{-/-}$), WT or CSE$^{-/-}$ male mice randomly treated with 4g/L STS in the water bottle were submitted to focal carotid artery stenosis to induce IH. Human vein segments were maintained in culture for 7 days to induce IH. Further *in vitro* studies were conducted in primary human vascular smooth muscle cell (VSMC).

Findings

STS inhibited IH in mice and in human vein segments. STS inhibited cell proliferation in the carotid artery wall and in human vein segments. STS increased polysulfides *in vivo* and protein persulfidation *in vitro,* which correlated with microtubule depolymerization, cell cycle arrest and reduced VSMC migration and proliferation.

Interpretation

STS, a drug used for the treatment of cyanide poisoning and calciphylaxis, protects against IH in a mouse model of arterial restenosis and in human vein segments. STS acts as an H_2S donor to limit VSMC migration and proliferation via microtubule depolymerization.
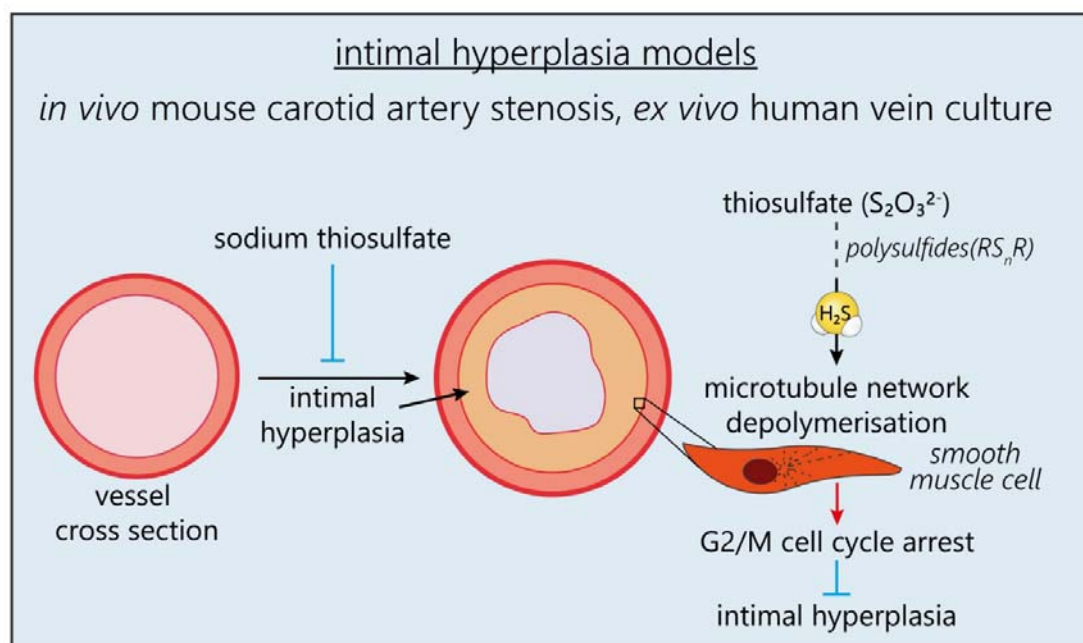
Funding

57   **Graphical Abstract**

58

59   **Abbreviations**

60   CAS: carotid artery stenosis

61   H_2S: hydrogen sulfide

62   IH: intimal hyperplasia

63   NaHS: sodium hydrogen sulfur

64   PCNA: proliferating cell nuclear antigen

65   SBP: systolic blood pressure

66   STS: Sodium Thiosulfate

67   VSMC: vascular smooth muscle cells

68   VGEL: Van Gieson elastic lamina

69

70 **Research in context**

71 **Evidence before this study**

72 Intimal hyperplasia (IH) is a complex process leading to vessel restenosis, a major
73 complication following cardiovascular surgeries and angioplasties. Therapies to limit IH are
74 currently limited. Pre-clinical studies suggest that hydrogen sulfide (H_2S), an endogenous
75 gasotransmitter, limits restenosis. However, despite these potent cardiovascular benefits in
76 pre-clinical studies, H_2S-based therapeutics are not available yet. Sodium thiosulfate
77 ($Na_2S_2O_3$) is an FDA-approved drug used for the treatment of cyanide poisoning and
78 calciphylaxis, a rare condition of vascular calcification affecting patients with end-stage renal
79 disease. Evidence suggest that thiosulfate may generate H_2S *in vivo* in pre-clinical studies.

80

81 **Added value of this study**

82 Here, we demonstrate that STS inhibit IH in a surgical mouse model of IH and in an *ex vivo*
83 model of IH in human vein culture. We further found that STS increases circulating
84 polysulfide levels *in vivo* and inhibits IH via decreased cell proliferation via disruption of the
85 normal cell's cytoskeleton. Finally, using CSE knockout mice, the main enzyme responsible
86 for H_2S production in the vasculature, we found that STS rescue these mice from accelerated
87 IF formation.

88 **Implications of all the available evidence**

89 These findings suggest that STS holds strong translational potentials to limit IH following
90 vascular surgeries and should be investigated further.

91

92

1. Introduction

94 Prevalence of peripheral arterial disease continues to rise worldwide, largely due to the combination of
95 aging, smoking, hypertension, and diabetes mellitus (1-3). Vascular surgery, open or endo, remains the best
96 treatment. However, the vascular trauma associated with the intervention eventually lead to restenosis and
97 secondary occlusion of the injured vessel. Re-occlusive lesions result in costly and complex recurrent end-organ
98 ischemia, and often lead to loss of limb, brain function, or life. Despite the advent of new medical devices such
99 as drug eluting stent and drug-coated balloons, restenosis has been delayed rather than suppressed (4), and
100 limited therapies are currently available.

101 Restenosis is mainly due to intimal hyperplasia (IH), a process instated by endothelial
102 cell injury and inflammation, which induces vascular smooth muscle cell (VSMC)
103 reprogramming. VSMCs become proliferative and migrating, secrete extra-cellular matrix and
104 form a new layer called the neo-intima, which slowly reduces the vessel luminal diameter (5).

105 Hydrogen sulfide (H_2S) is an endogenously produced gasotransmitter derived from
106 cysteine metabolism (6). Circulating H_2S levels are reduced in humans suffering from
107 vascular occlusive disease (7, 8) and pre-clinical studies using water-soluble sulfide salts
108 such as Na_2S and NaHS have shown that H_2S has cardiovascular protective properties(6),
109 including reduction of IH *in vivo* in rats (9), rabbits (10), mice (11), and *ex-vivo* in human vein
110 segments (12). However, the fast and uncontrolled release, narrow therapeutic range and
111 high salt concentration of these compounds limit their therapeutic potential. Due to these
112 limitations, H_2S-based therapy are currently not available.

113 Here, we focused on sodium thiosulfate ($Na_2S_2O_3$), an FDA-approved drug used in
114 gram-quantity doses for the treatment of cyanide poisoning(13) and calciphylaxis, a rare
115 condition of vascular calcification affecting patients with end-stage renal disease(14).
116 Pharmaceutical-grade sodium thiosulfate (STS) is available and has been suggested to
117 release H_2S through non-enzymatic and enzymatic mechanisms (15, 16).

118 We tested whether STS inhibit IH in a surgical mouse model of IH and in an *ex vivo*
119 model of IH in human vein culture. NaHS, a validated H_2S donor was systematically
120 compared to STS. We observed that STS was at least as potent as NaHS to inhibit IH in
121 mice carotids, and in human vein. Although STS did not release detectable amounts of H_2S
122 or polysulfides *in vitro*, it increased protein persulfidation and circulating polysulfide levels *in*
123 *vivo*. STS inhibited apoptosis and matrix deposition associated with the development of IH,
124 as well as VSMC proliferation and migration. We further observed that STS and NaHS
125 induced microtubule depolymerization in VSMCs.

126 **2. Methods**

127 For details on materials and reagents please see the Supplementary Material files

128 *2.1. Mouse treatment*

129 8 to 10 weeks old male WT or LDL receptor knock out (LDLR$^{-/-}$) mice on a C57BL/6J genetic
130 background were randomly divided into control vs sodium thiosulfate (STS) or NaHS.
131 Sodium Thiosulfate (Hänseler AG, Herisau, Switzerland) was given in mice water bottle at
132 4g/L (0.5g/Kg/day), changed 3 times a week. NaHS (Sigma-Aldrich) was given in mice water
133 bottle at 0.5g/L (125mg/Kg/day), changed every day. LDLR$^{-/-}$ mice were put on a cholesterol
134 rich diet (Western 1635, 0.2% Cholesterol, 21% Butter, U8958 Version 35, SAFE$^{®}$ Complete
135 Care Competence) for 3 weeks prior to experiments initiation. Mice were euthanized after 7
136 or 28 days of treatment by cervical dislocation under isoflurane anesthesia (inhalation 3%
137 isoflurane under 2.5 liter of O_2) followed by PBS perfusion. Aortas, carotid arteries, livers and
138 serum or plasma (via intracardiac blood collection with a 24G needle) were harvested.

139 *2.2. Cse$^{-/-}$ mice*

140 Cse knockout mice were generated from a novel floxed line generated by embryonic injection
141 of ES cells containing a Cth allele with LoxP sites flanking exon 2 (Cth
142 tm1a(EUCOMM)Hmgu). Both ES cells and recipient embryos were on C57BL/6J
143 background. Mice that were homozygous for the floxed allele were crossed with CMV-cre
144 global cre-expressing mice (B6.C-Tg(CMV-cre)1Cgn/J), which have been backcrossed with
145 C57BL/6J for 10 generations to create constitutive whole-body Cse$^{-/-}$ animals on a C57BL/6J
146 background. The line was subsequently maintained by breeding animals heterozygous for
147 the Cse null allele. Mouse ear biopsies were taken and digested in DirectPCR lysis reagent
148 (Viagen Biotech, 102-T) with proteinase K (Qiagen, 1122470). WT, heterozygous and
149 knockout mice were identified by PCR using the forward primer 5'-AGC ATG CTG AGG AAT
150 TTG TGC-3' and reverse primer 5'-AGT CTG GGG TTG GAG GAA AAA-3' to detect the WT
151 allele and the forward primer 5'-TTC AAC ATC AGC CGC TAC AG-3' to detect knock-out
152 allele using the platinum Taq DNA Polymerase (Invitrogen, cat#10966-026)

153

154 *2.3. Carotid artery stenosis (CAS) surgery*

155 The carotid artery stenosis (CAS) was performed as previously published (17) on 8 to 10
156 week old male WT or LDLR$^{-/-}$ mice. Treatment was initiated 3 days before surgery and
157 continued for 28 days post-surgery until organ collection. The day of the surgery, mice were
158 anesthetized with an intraperitoneal injection of Ketamine (80mg/kg) (Ketasol-100, Gräub
159 E.Dr.AG, Bern Switzerland) and Xylazine (15 mg/kg) (Rompun®, Provet AG, Lyssach,
160 Switzerland). The left carotid artery was exposed and separated from the jugular vein and
161 vagus nerve. Then, a 7.0 PERMA silk (Johnson & Johnson AG, Ethicon, Zug, Switzerland)
162 thread was looped and tightened around the carotid in presence of a 35-gauge needle. The
163 needle was removed, thereby restoring blood flow, albeit leaving a significant stenosis. The
164 stenosis triggers IH proximal to the site of injury, which was measured 28 days post surgery
165 (17). Buprenorphine (0.05 mg/kg Temgesic, Reckitt Benckiser AG, Switzerland) was
166 provided subcutaneously as post-operative analgesic every 12 hours for 24 hours. Mice were
167 euthanized under isoflurane anesthesia (inhalation 3% isoflurane under 2.5 liter of O_2) by
168 cervical dislocation and exsanguination, perfused with PBS followed by buffered formalin 4%
169 through the left ventricle. Surgeons were blind to the group during surgeries.

170 *2.4. Human tissue and VSMC culture*

171 Static vein culture was performed as previously described (12, 18). Briefly, the vein was cut
172 in 5 mm segments randomly distributed between conditions. One segment (D0) was
173 immediately preserved in formalin or flash frozen in liquid nitrogen and the others were

174 maintained in culture for 7 days in RPMI-1640 Glutamax I supplemented with 10 % FBS and
175 1% antibiotic solution (10,000 U/mL penicillin G, 10,000 U/mL streptomycin sulfate) in cell
176 culture incubator at 37°C, 5% CO_2 and 21% O_2.

177 Human VSMCs were also prepared from these human great saphenous vein segments as
178 previously described (12, 18) . Vein explants were plated on the dry surface of a cell culture
179 plate coated with 1% Gelatin type B (Sigma-Aldrich). Explants were maintained in RPMI,
180 10% FBS medium in a cell culture incubator at 37°C, 5% CO_2, 5% O_2 environment.

181 *2.5. Carotid and human vein histomorphometry*

182 After 7 days in culture, or immediately upon vein collection (D0), the vein segments were
183 fixed in buffered formalin, embedded in paraffin, cut into 5 μm sections, and stained using
184 Van Gieson Elastic Laminae (VGEL) staining as previously described (12, 19). Three
185 photographs per section were taken at 100x magnification and 8 measurements of the intima
186 and media thicknesses were made, evenly distributed along the length of the vein wall.

187 Left ligated carotids were isolated and paraffin-embedded. Six-μm sections of the ligated
188 carotid artery were cut from the ligature towards the aortic arch and stained with VGEL for
189 morphometric analysis. Cross sections at every 300 μm and up to 2 mm from the ligature
190 were analyzed using the Olympus Stream Start 2.3 software (Olympus, Switzerland). For
191 intimal and medial thickness, 72 (12 measurements/cross section on six cross sections)
192 measurements were performed, as previously described (12).

193 Two independent researchers blind to the experimental groups did the morphometric
194 measurements, using the Olympus Stream Start 2.3 software (Olympus, Switzerland) (12).

195 *2.6. H_2S and polysulfide measurement*

196 Free H_2S was measured in cells using the SF_7-AM fluorescent probe (20) (Sigma-Aldrich).
197 The probe was dissolved in anhydrous DMF at 5 mM and used at 5 μM in serum-free RPMI
198 medium with or without VSMCs. Free polysulfide was measured in cells using the SSP4
199 fluorescent probe. The probe was dissolved in DMF at 10 mM and diluted at 10 μM in serum-
200 free RPMI medium with or without VSMCs. Fluorescence intensity (λ_{ex} = 495 nm; λ_{em} = 520
201 nm) was measured continuously in a Synergy Mx fluorescent plate reader (BioTek
202 Instruments AG, Switzerland) at 37 °C before and after addition of various donors, as
203 indicated.

204 Plasma polysulfides were measured using the SSP4 fluorescent probe. Plasma samples
205 were diluted 3 times and incubated for 10 min at 37°C in presence of 10 μM SSP4. Plasma
206 polysulfides were calculated using a Na_2S_3 standard curve. Liver polysulfides were measured
207 using the SSP4 fluorescent probe. Pulverized frozen liver was resuspended in PBS-0.5%
208 triton X-100, sonicated and adjusted to 0.5 mg/ml protein concentration. Lysates were
209 incubated for 15 min at 37°C in presence of 10 μM SSP4 and fluorescence intensity (λ_{ex} =
210 495 nm; λ_{em} = 520 nm) was measured in a Synergy Mx fluorescent plate reader (BioTek
211 Instruments AG, Switzerland)

212 *2.7. Persulfidation protocol*

213 Persulfidation protocol was performed using a dimedone-based probe as recently described
214 (21). Persulfidation staining was performed on VSMCs grown on glass coverslips. Briefly,
215 1mM 4-Chloro-7-nitrobenzofurazan (NBF-Cl, Sigma) was diluted in PBS and added to live
216 cells for 20 minutes. Cells were washed with PBS then fixed for 10 minutes in ice-cold
217 methanol. Coverslips were rehydrated in PBS, and incubated with 1mM NBF-Cl for 1h at
218 37°C. Daz2-Cy5.5 (prepared with 1mM Daz-2, 1mM alkyne Cy5.5, 2mM copper(II)-TBTA,
219 4mM ascorbic acid with overnight incubation at RT, followed by quenching for 1h with 20mM
220 EDTA) was added to the coverslips and incubated at 37°C for 1h. After washing with
221 methanol and PBS, coverslips were mounted in Vectashield mounting medium with DAPI
222 and visualized with a 90i Nikon fluorescence microscope.

2.8. BrdU assay

223
224 VSMC were grown at 80% confluence ($5 \cdot 10^3$ cells per well) on glass coverslips in a 24-well
225 plate and starved overnight in serum-free medium. Then, VSMC were either treated or not
226 (ctrl) with the drug of choice for 24 hours in full medium (RPMI 10% FBS) in presence of
227 10µM BrdU. All conditions were tested in parallel. All cells were fixed in ice-cold methanol
228 100% after 24 hours of incubation and immunostained for BrdU. Images were acquired using
229 a Nikon Eclipse 90i microscope. BrdU-positive nuclei and total DAPI-positive nuclei were
230 automatically detected using the ImageJ software (12).

2.9. Flow Cytometry

231
232 VSMC were grown at 70% confluence ($5 \cdot 10^4$ cells per well) and treated for 48 hours with
233 15mM STS or 10nM Nocodazole. Then, cells were tripsinized, collected and washed in ice-
234 cold PBS before fixation by dropwise addition of ice-cold 70% ethanol while slowly vortexing
235 the cell pellet. Cells were fixed for 1 hour at 4°C, washed 3 times in ice-cold PBS and
236 resuspended in PBS supplemented with 20µg/mL RNAse A and 10µg/mL DAPI. Flow
237 cytometry was performed in a Cytoflex-S apparatus (Beckmann).

2.10. Wound healing assay

238
239 VSMC were grown at confluence (10^4 cells per well) in a 12-well plate and starved overnight
240 in serum-free medium. Then, a scratch wound was created using a sterile p200 pipette tip
241 and medium was changed to full medium (RPMI 10% FBS). Repopulation of the wounded
242 areas was recorded by phase-contrast microscopy over 24 hours in a Nikon Ti2-E live cell
243 microscope. All conditions were tested in parallel. The area of the denuded area was
244 measured at t=0 hours and t=10 hours after the wound using the ImageJ software by two
245 independent observers blind to the conditions. Data were expressed as a ratio of the healed
246 area over the initial wound area.

2.11. Apoptosis assay

247
248 Apoptosis TUNEL assay was performed using the DeadEnd^{TM} Fluorometric TUNEL system
249 kit (Promega) on frozen sections of human vein segments. Immunofluorescent staining was
250 performed according to the manufacturer's instruction. Apoptotic nuclei were automatically
251 detected using the ImageJ software and normalized to the total number of DAPI-positive
252 nuclei. *In vitro* VSMC apoptosis was determined by hoescht/propidium iodide staining of live
253 VSMC and manually counted by two independent blinded experimenters (22).

2.12. Immunohistochemistry

254
255 *Polychrome Herovici staining* was performed on paraffin sections as described (23). Young
256 collagen is stained blue, while mature collagen is pink. Cytoplasm is counterstained yellow.
257 Hematoxylin is used to counterstain nuclei blue to black.

258 *Collagen III staining* was performed on frozen sections (OCT embedded) of human vein
259 segments using mouse anti-Collagen III antibody (ab7778, abcam). Briefly, tissue slides
260 were permeabilized in PBS supplemented with 2 wt. % BSA and 0.1 vol. % Triton X-100 for
261 30 min, blocked in PBS supplemented with 2 wt. % BSA and 0.1 vol. % Tween 20 for another
262 30 min, and incubated overnight with the primary antibodies diluted in the same buffer. The
263 slides were then washed 3 times for 5 min in PBS supplemented with 0.1 vol. % Tween 20,
264 and incubated for 1 hour at room temperature with anti-mouse AlexaFluor 568 (1/1000,
265 ThermoFischer). Slides were visualized using a Nikon 90i fluorescence microscope (Nikon
266 AG). Collagen III immunostaining area was quantified using the ImageJ software and
267 normalized to the total area of the vein segment.

268 *PCNA (proliferating cell nuclear antigen) and α-tubulin immunohistochemistry* was performed
269 on paraffin sections as previously described (24). After rehydration and antigen retrieval
270 (TRIS-EDTA buffer, pH 9, 17 min in a microwave at 500 watts), immunostaining was

271 performed on human vein or carotid sections using the EnVision +/HRP, DAB+ system
272 according to manufacturer's instructions (Dako, Baar, Switzerland). Slides were further
273 counterstained with hematoxylin. PCNA and hematoxylin positive nuclei were manually
274 counted by two independent observers blinded to the conditions.

275 *α-tubulin immunofluorescent staining* in human VSMC was performed as previously
276 described. Cell were fixed at -20°C for 10min in absolut methanol. Then, cell were
277 blocked/permeabilized in PBS- triton 0.2%, BSA 3% for 45 min at room temperature. Cells
278 were incubated overnight at 4°C in the primary antibody diluted in PBS-0.1% tween, 3%
279 BSA, washed 3 times in PBS and incubated for 1 hour at room temperature with the
280 secondary antibody diluted in PBS-0.1% tween, 3% BSA, washed again 3 times in PBS and
281 mounted using Vectashield mounting medium for fluorescence with DAPI. The microtubule
282 staining was quantified automatically using FiJi (ImageJ, 1.53c). Image processing was as
283 follows: Plugin, Tubeness/Process, Make Binary/Analyze, Skeleton. Data were summarized
284 as filament number and total length, normalized to the number of cells per images. Data
285 were generated from images from 3 independent experiments, 3 to 4 images per experiment
286 per condition.

2.13. Western blotting

288 Mice aortas or human vein segments were flash-frozen in liquid nitrogen, grinded to power
289 and resuspended in SDS lysis buffer (62.5 mM TRIS pH6,8, 5% SDS, 10 mM EDTA). Protein
290 concentration was determined by DC protein assay (Bio-Rad Laboratories, Reinach,
291 Switzerland). 10 to 20 µg of protein were loaded per well. Primary cells were washed once
292 with ice-cold PBS and directly lysed with Laemmli buffer as previously described (12, 18).
293 Lysates were resolved by SDS-PAGE and transferred to a PVDF membrane (Immobilon-P,
294 Millipore AG, Switzerland). Immunoblot analyses were performed as previously
295 described(18) using the antibodies described in supplementary Table S1**.** Membranes were
296 revealed by enhanced chemiluminescence (Immobilon, Millipore) using the Azure
297 Biosystems 280 and analyzed using Image J. Protein abundance was normalized to total
298 protein using Pierce™ Reversible Protein Stain Kit for PVDF Membranes.

2.14. In vitro tubulin polymerization assay

300 The assay was performed using the *In Vitro* Tubulin Polymerization Assay Kit (≥99% Pure
301 Bovine Tubulin; 17-10194 Sigma-Aldrich), according to the manufacturer's instruction.

2.15. Statistical analyses

303 All experiments adhered to the ARRIVE guidelines and followed strict randomization. A
304 power analysis was performed prior to the study to estimate sample-size. We hypothesized
305 that STS would reduce IH by 50%. Using an SD at +/- 20% for the surgery and considering a
306 power at 0.9, we calculated that n= 12 animals/group was necessary to validate a significant
307 effect of the STS. All experiments were analyzed using GraphPad Prism 8. One or 2-ways
308 ANOVA were performed followed by multiple comparisons using post-hoc t-tests with the
309 appropriate correction for multiple comparisons.

2.16. Role of funding source

311 The funding sources had no involvement in study design, data collection, data analyses,
312 interpretation, or writing of report.

2.17. Ethics Statement

314 Human great saphenous veins were obtained from donors who underwent lower limb bypass
315 surgery (25). Written, informed consent was obtained from all vein donors for human vein
316 and VSMC primary cultures. The study protocols for organ collection and use were reviewed
317 and approved by the Centre Hospitalier Universitaire Vaudois (CHUV) and the Cantonal

318   Human Research Ethics Committee (http://www.cer-vd.ch/, no IRB number, Protocol Number
319   170/02), and are in accordance with the principles outlined in the Declaration of Helsinki of
320   1975, as revised in 1983 for the use of human tissues.

321   All animal experimentations conformed to *the National Research Council:* Guide for the Care
322   and Use of Laboratory Animals (26). All animal care, surgery, and euthanasia procedures
323   were approved by the CHUV and the Cantonal Veterinary Office (SCAV-EXPANIM,
324   authorization number 3114, 3258 and 3504).

325

326

327   ## 3. Results

328   ### *3.1. STS limits IH development in mice after carotid artery stenosis*

329   We first assessed whether STS protects against IH, 28 days after carotid artery stenosis in
330   mice (CAS)(17). STS treatment (4g/L) decreased IH by about 50% in WT mice (**Figure 1A**),
331   as expressed as the mean intima thickness, the ratio of intima over media thickness (I/M), or
332   the area under the curve of intima thickness calculated over 1 mm. To model the
333   hyperlipidaemic state of patients with PAD, we also performed the CAS on
334   hypercholesterolemic LDLR$^{-/-}$ mice fed for 3 weeks with a cholesterol-rich diet. As expected,
335   the LDLR$^{-/-}$ mice developed more IH than WT mice upon CAS, and STS treatment lowered
336   IH by about 70% (**Figure 1B**). Interestingly, STS did not reduce media thickness in WT mice
337   (p= but significantly reduced media thickness in LDLR$^{-/-}$ mice (p=**Figure 1B**). Of note, the
338   sodium salt H_2S donor NaHS (0.5g/L) also significantly decreased IH following carotid
339   stenosis in WT mice (**Figure S1 in the online supplementary files)**.

340   ### *3.2. STS limits IH development in a model of ex vivo human vein segment culture*

341   Both STS (15mM) and NaHS (100µM) inhibited IH development in our validated model of
342   static *ex vivo* human vein segment culture(12) as measured by intima thickness and I/M ratio
343   (**Figure 1C**). The polysulfide/H_2S donors diallyl trisulfide (DATS), cysteine-activated donor 5a
344   and GYY4137 also prevented the development of IH in human vein segments (**Figure S2).**

345   ### *3.3. STS is a biologically active source of sulfur*

346   Overall, STS and "classical" H_2S donors similarly inhibit IH. To measure whether STS
347   releases detectable amounts of H_2S or polysulfides, we used the SF_7-AM and SSP4 probes,
348   respectively. We could not detect any increase in SSP4 or SF_7-AM fluorescence in presence
349   of STS with or without VSMCs. Na_2S_3 was used as a positive control for the SSP4 probe and
350   NaHS as a positive control for the SF_7-AM probe (**Figure S3).** The biological activity of H_2S is
351   mediated by post-translational modification of reactive cysteine residues by persulfidation,
352   which influence protein activity (21, 27). As a proxy for H_2S release, we assessed global
353   protein persulfidation by DAZ-2-Cy5.5 labelling of persulfide residues in VSMC treated for 4
354   hours with NaHS or STS. Both STS and NaHS similarly increased persulfidation in VSMC
355   (**Figure 2A**). Using the SSP4 probe, we further observed higher polysulfides levels *in vivo* in
356   the plasma of mice treated for 1 week with 4g/L STS (**Figure 2B**). Similarly, polysulfides
357   levels tended to be higher in the liver of mice treated with STS (p=0.15). As a positive
358   control, mice treated with 0.5g/L NaHS had significantly higher polysulfides levels in the liver
359   (**Figure 2C**). Cse is main enzyme responsible for endogenous H_2S in the vasculature and
360   Cse$^{-/-}$ mice have been shown to develop more IH (11, 28, 29). Here, we generated a new
361   Cse knock-out mouse line. Consistent with a role as an H_2S donor, STS fully rescued Cse$^{-/-}$
362   mice from increased IH in the model of carotid artery stenosis (**Figure 2D**).

363   ### *3.4. STS limits IH-associated matrix deposition and apoptosis in human vein segments*

364   We further assessed matrix deposition and apoptosis in human vein segments. Concomitant
365   with IH formation, *ex vivo* vein culture (D7) resulted in *de novo* collagen deposition compared
366   to D0, as assessed by polychrome Herovici staining (**Figure 3A)**. Immunoanalysis of
367   immature Collagen III levels confirmed that vein culture (D7) resulted in *de novo* collagen
368   deposition compared to D0, as assessed by Western blot (**Figure 3B)** and immunostaining
369   (**Figure 3C).** STS and NaHS treatment tended to reduce collagen deposition as assessed by
370   Herovici staining, collagen III immunostaining and Western blotting (**Figure 3A-C).** TUNEL
371   assay revealed that STS, and to a lesser degree NaHS, decreased the percentage of
372   apoptotic cells observed after 7 days in culture (D7) (**Figure 3D)**. STS also attenuated pro-
373   apoptotic protein Bax overexpression observed after 7 days in culture, while NaHS had a
374   non-significant tendency to decrease Bax level (p=.11; **Figure 3E**). STS also tended to

11

375 increase the protein level of anti-apoptotic protein Bcl-2 (p=.06), while NaHS significantly
376 increased it (p=.04; **Figure 3E**).

377   *3.5. STS blocks VSMC proliferation and migration*

378 IH is driven by VSMC reprogramming toward a proliferating, migrating and ECM-secreting
379 phenotype (5). Both STS and NaHS significantly reduced the percentage of proliferating cells
380 (defined as PCNA positive nuclei over total nuclei) *in vivo* in CAS-operated carotids in WT
381 mice (**Figure 4A**) and *ex vivo* in human vein segments (**Figure 4B**). *In vitro,* STS dose-
382 dependently decreased primary human VSMC proliferation as assessed by BrdU
383 incorporation assay (**Figure 5A**). Of Note, NaHS as well as DATS, donor5A and GYY4137,
384 also decreased VSMC proliferation (**Figure S4**). STS and NaHS also decreased VSMC
385 migration in a wound healing assay (**Figure 5B**). Further evaluation of cell morphology
386 during the wound healing revealed that STS and NaHS-treated cells lost the typical
387 elongated shape of VSMC, as measured through the area, Feret diameter and circularity of
388 the cells (**Figure 5C**).

389   *3.6. STS interferes with microtubules organization*

390 Given the impact of STS on cell morphology, we examined in more details the effect of STS
391 on the cell cytoskeleton. α-tubulin levels were increased in the carotid wall of CAS-operated
392 mice, which were reduced by STS, as demonstrated by immunohistochemistry (**Figure 6A**).
393 α-tubulin levels were also decreased in the native aorta of mice treated with STS for 7 days
394 (**Figure 6B**). Similarly, total α-tubulin levels were decreased in *ex vivo* vein segments after 7
395 days of STS treatment (**Figure 6C-D**). Looking further at α-tubulin by immunofluorescent
396 staining showed a loss in microtubule in VSMCs treated with STS or NaHS for 8 hours
397 (**Figure 6 E-F**). To study the effect of H_2S on microtubule formation, an *in vitro* tubulin
398 polymerization assay was performed in presence of 15mM STS, 100 μM NaHS or 10μM
399 Nocodazole, an inhibitor of microtubule assembly. As expected, Nocodazole slowed down
400 microtubule assembly, as compared to the control. Surprisingly, both NaHS and STS fully
401 blocked microtubule assembly in this assay (**Figure 6G**). Further studies of the cell cycle in
402 VSMC revealed that 48 hours of treatment with STS or Nocodazole resulted in accumulation
403 of cells in G2/M phase (**Figure 6H**).

404

Discussion

Despite decades of research, intimal hyperplasia remains one of the major limitations in the long-term success of revascularization. In addition, in December 2018, Katsanos and colleagues reported, in a systematic review and meta-analysis, an increased risk of all-cause mortality following application of paclitaxel-coated balloons and stents in the femoropopliteal artery (30). This recent report had tremendous repercussions on the community, urging vascular societies and policy makers to further investigate the use of paclitaxel-coated balloons, stents and other devices for the treatment of peripheral arterial disease. Here, we demonstrate that exogenous sulfur supplementation in the form of STS limits IH development *in vivo* following mouse carotid artery stenosis. Furthermore, STS reduced apoptosis, vessel remodeling and collagen deposition, along with IH development in our *ex vivo* model of IH in human vein segments. We propose that STS limits IH by interfering with the microtubule dynamics, thus VSMC proliferation and migration.

An ever increasing number of studies document the protective effects of H_2S against cardiovascular diseases (31), including studies showing that H_2S reduces IH in preclinical models (9-11, 32). The administration of H_2S in those studies relies on soluble sulfide salts such as NaHS with narrow therapeutic range due to fast and uncontrolled release. Thiosulfate is an intermediate of sulfur metabolism that can lead to the production of H_2S (15, 33, 34). Importantly, STS is clinically approved and safe in gram quantities in humans. Although STS yields no detectable H_2S or polysulfide *in vitro*, we observed increased circulating and liver levels of polysulfides in mice, as well as increased protein persulfidation in VSMC. Overall, STS has protective effects against IH similar to the H_2S salt NaHS and several other "classical" H_2S donors, but holds much higher translational potential.

Mechanistically, we first observed that STS reduces cell apoptosis and matrix deposition in our *ex vivo* model of human vein segments. This anti-apoptotic effect of STS and NaHS is in line with known anti-apoptotic effects of H_2S (31). STS also reduces IH *in vivo* following carotid artery stenosis. In this model, fibrosis plays little role in the formation of IH, which relies mostly on VSMC proliferation (5). Therefore, although ECM and especially collagen deposition are major features of IH in human (35, 36), reduced apoptosis and matrix deposition is not sufficient to fully explain the protection afforded by STS in carotids *in vivo*.

STS, similarly to the H_2S donor NaHS, also inhibits VMSC proliferation and migration in the context of IH *in vivo* in mouse stenotic carotids, as well as *ex vivo* in human vein segments, and *in vitro* in primary human VSMC. These findings are in line with previous studies demonstrating that "classical" H_2S donors decrease VSMCs proliferation in pre-clinical models (10, 12, 37). In mouse VSMC, exogenous H_2S has been proposed to promote cell cycle arrest (28), and regulate the MAPK pathway (9) and IGF-1 response (38). Regarding mouse VSMC migration, H_2S may limit α5β1-integrin and MMP2 expression, preventing migration and ECMs degradation (11, 28).

In this study, we further document that STS and NaHS disrupt the formation of microtubules in human VSMC *in vitro*. Our findings are in line with previous studies showing that Diallyl trisulfide, a polysulfide donor, inhibits microtubule polymerization to block human colon cancer cell proliferation (39). NaHS also depolymerizes microtubules within Aspergillus nidulans biofilms (40). The α/β tubulin dimer has 20 highly conserved cysteine residues, which have been shown to regulate microtubule formation and dynamics (41). In particular, thiol–disulfide exchanges in intrachain disulfide bonds have been proposed to play a key role in microtubule assembly (42). Several high throughput studies of post-translational modification of protein cysteinyl thiols (-SH) to persulfides (-SSH) demonstrated that cysteine residues in α- and β-tubulin are persulfidated in response to H_2S donors in various cell types (43, 44). Given the prominent role of cytoskeleton dynamics and remodelling during mitosis and cell migration, we propose that STS/H_2S-driven microtubule depolymerisation, secondary to cysteine persulfidation, contributes to cell cycle arrest and reduces migration in VSMC.

456 Our findings suggest that STS holds strong translational potential to limit restenosis
457 following vascular surgeries. The dosage of STS used in this study is comparable to previous
458 experimental studies using 0.5 to 2 g/Kg/day (15, 16, 33, 34). In humans, 12.5 and 25 g of
459 STS has been infused without adverse effects (45) and short-term treatment with i.v. STS is
460 safely used in patients for the treatment of calciphylaxis (14). Of note, the pathophysiology of
461 calciphylaxis, also known as calcific uremic arteriopathy (CUA), is caused by oxidative stress
462 and inflammation, which promote endothelial dysfunction, leading to medial remodelling,
463 inflammation, fibrosis and VSMC apoptosis and differentiation into bone forming osteoblast-
464 like cells. Although the main effect of STS on CUA is certainly the formation of highly soluble
465 calcium thiosulfate complexes, our data certainly support the positive effects of STS in the
466 treatment of calciphylaxis. Plus, STS infusions have been shown to increase distal
467 cutaneous blood flow, which could be beneficial in the context of vascular occlusive disease.

468 Here, we propose that STS treatment results in persulfidation of cysteine residues in
469 the tubulin proteins, which lead to microtubule depolymerization. However, further studies
470 are required to test this hypothesis and demonstrate the STS-induced persulfidation of
471 tubulin cysteine residues. In addition, although we show *in vitro* that H_2S directly affect
472 microtubule formation in a cell-free environment, other proteins involved in the microtubules
473 dynamics *in vivo* may also be modified by H_2S, and contribute to the effect of STS on
474 microtubule polymerization and cell proliferation. In this study, STS was administered in the
475 water bottle. However, a validated oral form of the compound has not been developed yet.
476 Case reports and case series suggest that intravenous STS administration is safe, even for
477 relatively long periods of time (46, 47). However, randomized controlled trials testing long-
478 term administration of STS are lacking (47) and the long-term safety and effects of STS
479 administration should be further explored.

480 In summary, under the conditions of these experiments, STS, a FDA-approved
481 compound, limits IH development *in vivo* in a model of arterial restenosis and *ex vivo* model
482 in human veins. STS most likely acts by increasing H_2S bioavailability, which inhibits cell
483 apoptosis and matrix deposition, as well as VSMC proliferation and migration via
484 microtubules depolymerization.

485

486

487 **Contributors**

488 FA, AL and SD designed the study. FA, DM, MMA, ML and SU performed the experiments.
489 FA, DM, MMA, ML and SD analyzed the data. FA, DM, MMA, AL and SD wrote the
490 manuscript. JMC critically revised the manuscript. FA, AL, SD and DM finalized the
491 manuscript.

492 **Funding**

496

497 **Data sharing statement**

498 The data that support the findings of this study are available from the corresponding author,
499 Florent Allagnat, upon request.

500

501 **Declaration of Competing Interest**

502 The authors declare no competing interests.

503 **Acknowledgments**

506
507
508

509 **References**

510 1.   Eraso LH, Fukaya E, Mohler ER, 3rd, Xie D, Sha D, Berger JS. Peripheral arterial
511 disease, prevalence and cumulative risk factor profile analysis. European journal of
512 preventive cardiology. 2014;21(6):704-11.
513 2.   Fowkes FG, Rudan D, Rudan I, Aboyans V, Denenberg JO, McDermott MM, et al.
514 Comparison of global estimates of prevalence and risk factors for peripheral artery disease in
515 2000 and 2010: a systematic review and analysis. Lancet. 2013;382(9901):1329-40.
516 3.   Song P, Rudan D, Zhu Y, Fowkes FJI, Rahimi K, Fowkes FGR, et al. Global, regional, and
517 national prevalence and risk factors for peripheral artery disease in 2015: an updated
518 systematic review and analysis. Lancet Glob Health. 2019;7(8):e1020-e30.
519 4.   Jukema JW, Verschuren JJ, Ahmed TA, Quax PH. Restenosis after PCI. Part 1:
520 pathophysiology and risk factors. Nat Rev Cardiol. 2011;9(1):53-62.
521 5.   Davies MG, Hagen PO. Reprinted article "Pathophysiology of vein graft failure: a
522 review". Eur J Vasc Endovasc Surg. 2011;42 Suppl 1:S19-29.
523 6.   Zhang L, Wang Y, Li Y, Li L, Xu S, Feng X, et al. Hydrogen Sulfide (H2S)-Releasing
524 Compounds: Therapeutic Potential in Cardiovascular Diseases. Front Pharmacol.
525 2018;9:1066.
526 7.   Islam KN, Polhemus DJ, Donnarumma E, Brewster LP, Lefer DJ. Hydrogen Sulfide
527 Levels and Nuclear Factor-Erythroid 2-Related Factor 2 (NRF2) Activity Are Attenuated in the
528 Setting of Critical Limb Ischemia (CLI). J Am Heart Assoc. 2015;4(5).
529 8.   Longchamp A, MacArthur MR, Trocha K, Ganahl J, Mann CG, Kip P, et al. Plasma
530 Hydrogen Sulfide Production Capacity is Positively Associated with Post-Operative Survival in
531 Patients Undergoing Surgical Revascularization. 2021:2021.02.16.21251804.

532   9.   Meng QH, Yang G, Yang W, Jiang B, Wu L, Wang R. Protective effect of hydrogen
533   sulfide on balloon injury-induced neointima hyperplasia in rat carotid arteries. Am J Pathol.
534   2007;170(4):1406-14.
535   10.   Ma B, Liang G, Zhang F, Chen Y, Zhang H. Effect of hydrogen sulfide on restenosis of
536   peripheral arteries after angioplasty. Mol Med Rep. 2012;5(6):1497-502.
537   11.   Yang G, Li H, Tang G, Wu L, Zhao K, Cao Q, et al. Increased neointimal formation in
538   cystathionine gamma-lyase deficient mice: role of hydrogen sulfide in alpha5beta1-integrin
539   and matrix metalloproteinase-2 expression in smooth muscle cells. J Mol Cell Cardiol.
540   2012;52(3):677-88.
541   12.   Longchamp A, Kaur K, Macabrey D, Dubuis C, Corpataux JM, Deglise S, et al.
542   Hydrogen sulfide-releasing peptide hydrogel limits the development of intimal hyperplasia in
543   human vein segments. Acta Biomater. 2019.
544   13.   Bebarta VS, Brittain M, Chan A, Garrett N, Yoon D, Burney T, et al. Sodium Nitrite and
545   Sodium Thiosulfate Are Effective Against Acute Cyanide Poisoning When Administered by
546   Intramuscular Injection. Ann Emerg Med. 2017;69(6):718-25 e4.
547   14.   Nigwekar SU, Thadhani R, Brandenburg VM. Calciphylaxis. N Engl J Med.
548   2018;378(18):1704-14.
549   15.   Olson KR, Deleon ER, Gao Y, Hurley K, Sadauskas V, Batz C, et al. Thiosulfate: a readily
550   accessible source of hydrogen sulfide in oxygen sensing. Am J Physiol Regul Integr Comp
551   Physiol. 2013;305(6):R592-603.
552   16.   Snijder PM, Frenay AR, de Boer RA, Pasch A, Hillebrands JL, Leuvenink HG, et al.
553   Exogenous administration of thiosulfate, a donor of hydrogen sulfide, attenuates
554   angiotensin II-induced hypertensive heart disease in rats. Br J Pharmacol. 2015;172(6):1494-
555   504.
556   17.   Tao M, Mauro CR, Yu P, Favreau JT, Nguyen B, Gaudette GR, et al. A simplified murine
557   intimal hyperplasia model founded on a focal carotid stenosis. Am J Pathol. 2013;182(1):277-
558   87.
559   18.   Allagnat F, Dubuis C, Lambelet M, Le Gal L, Alonso F, Corpataux JM, et al. Connexin37
560   reduces smooth muscle cell proliferation and intimal hyperplasia in a mouse model of
561   carotid artery ligation. Cardiovasc Res. 2017;113(7):805-16.
562   19.   Longchamp A, Alonso F, Dubuis C, Allagnat F, Berard X, Meda P, et al. The use of
563   external mesh reinforcement to reduce intimal hyperplasia and preserve the structure of
564   human saphenous veins. Biomaterials. 2014;35(9):2588-99.
565   20.   Lin VS, Lippert AR, Chang CJ. Cell-trappable fluorescent probes for endogenous
566   hydrogen sulfide signaling and imaging H2O2-dependent H2S production. Proc Natl Acad Sci
567   U S A. 2013;110(18):7131-5.
568   21.   Zivanovic J, Kouroussis E, Kohl JB, Adhikari B, Bursac B, Schott-Roux S, et al. Selective
569   Persulfide Detection Reveals Evolutionarily Conserved Antiaging Effects of S-Sulfhydration.
570   Cell Metab. 2019;30(6):1152-70 e13.
571   22.   Allagnat F, Fukaya M, Nogueira TC, Delaroche D, Welsh N, Marselli L, et al. C/EBP
572   homologous protein contributes to cytokine-induced pro-inflammatory responses and
573   apoptosis in beta-cells. Cell Death Differ. 2012;19(11):1836-46.
574   23.   Teuscher AC, Statzer C, Pantasis S, Bordoli MR, Ewald CY. Assessing Collagen
575   Deposition During Aging in Mammalian Tissue and in Caenorhabditis elegans. Methods Mol
576   Biol. 2019;1944:169-88.

577   24.   Allagnat F, Haefliger JA, Lambelet M, Longchamp A, Berard X, Mazzolai L, et al. Nitric
578   Oxide Deficit Drives Intimal Hyperplasia in Mouse Models of Hypertension. Eur J Vasc
579   Endovasc Surg. 2016;51(5):733-42.
580   25.   Dubuis C, May L, Alonso F, Luca L, Mylonaki I, Meda P, et al. Atorvastatin-loaded
581   hydrogel affects the smooth muscle cells of human veins. The Journal of pharmacology and
582   experimental therapeutics. 2013;347(3):574-81.
583   26.   National Research Council (U.S.). Committee for the Update of the Guide for the Care
584   and Use of Laboratory Animals., Institute for Laboratory Animal Research (U.S.), National
585   Academies Press (U.S.). Guide for the care and use of laboratory animals. 8th ed.
586   Washington, D.C.: National Academies Press; 2011. xxv, 220 p. p.
587   27.   Li Z, Polhemus DJ, Lefer DJ. Evolution of Hydrogen Sulfide Therapeutics to Treat
588   Cardiovascular Disease. Circ Res. 2018;123(5):590-600.
589   28.   Yang G, Wu L, Bryan S, Khaper N, Mani S, Wang R. Cystathionine gamma-lyase
590   deficiency and overproliferation of smooth muscle cells. Cardiovasc Res. 2010;86(3):487-95.
591   29.   Yuan S, Yurdagul A, Jr., Peretik JM, Alfaidi M, Al Yafeai Z, Pardue S, et al.
592   Cystathionine gamma-Lyase Modulates Flow-Dependent Vascular Remodeling. Arterioscler
593   Thromb Vasc Biol. 2018;38(9):2126-36.
594   30.   Katsanos K, Spiliopoulos S, Kitrou P, Krokidis M, Karnabatidis D. Risk of Death
595   Following Application of Paclitaxel-Coated Balloons and Stents in the Femoropopliteal Artery
596   of the Leg: A Systematic Review and Meta-Analysis of Randomized Controlled Trials. J Am
597   Heart Assoc. 2018;7(24):e011245.
598   31.   Szabo C. A timeline of hydrogen sulfide (H2S) research: From environmental toxin to
599   biological mediator. Biochem Pharmacol. 2018;149:5-19.
600   32.   Kip P, Tao M, Trocha KM, MacArthur MR, Peters HAB, Mitchell SJ, et al.
601   Periprocedural Hydrogen Sulfide Therapy Improves Vascular Remodeling and Attenuates
602   Vein Graft Disease. J Am Heart Assoc. 2020;9(22):e016391.
603   33.   Marutani E, Yamada M, Ida T, Tokuda K, Ikeda K, Kai S, et al. Thiosulfate Mediates
604   Cytoprotective Effects of Hydrogen Sulfide Against Neuronal Ischemia. J Am Heart Assoc.
605   2015;4(11).
606   34.   Lee M, McGeer EG, McGeer PL. Sodium thiosulfate attenuates glial-mediated
607   neuroinflammation in degenerative neurological diseases. J Neuroinflammation. 2016;13:32.
608   35.   Farb A, Kolodgie FD, Hwang JY, Burke AP, Tefera K, Weber DK, et al. Extracellular
609   matrix changes in stented human coronary arteries. Circulation. 2004;110(8):940-7.
610   36.   Suna G, Wojakowski W, Lynch M, Barallobre-Barreiro J, Yin X, Mayr U, et al.
611   Extracellular Matrix Proteomics Reveals Interplay of Aggrecan and Aggrecanases in Vascular
612   Remodeling of Stented Coronary Arteries. Circulation. 2018;137(2):166-83.
613   37.   Yang G, Wu L, Wang R. Pro-apoptotic effect of endogenous H2S on human aorta
614   smooth muscle cells. FASEB J. 2006;20(3):553-5.
615   38.   Shuang T, Fu M, Yang G, Wu L, Wang R. The interaction of IGF-1/IGF-1R and hydrogen
616   sulfide on the proliferation of mouse primary vascular smooth muscle cells. Biochem
617   Pharmacol. 2018;149:143-52.
618   39.   Hosono T, Hosono-Fukao T, Inada K, Tanaka R, Yamada H, Iitsuka Y, et al. Alkenyl
619   group is responsible for the disruption of microtubule network formation in human colon
620   cancer cell line HT-29 cells. Carcinogenesis. 2008;29(7):1400-6.
621   40.   Shukla N, Osmani AH, Osmani SA. Microtubules are reversibly depolymerized in
622   response to changing gaseous microenvironments within Aspergillus nidulans biofilms. Mol
623   Biol Cell. 2017;28(5):634-44.

624   41.   Britto PJ, Knipling L, McPhie P, Wolff J. Thiol-disulphide interchange in tubulin:
625   kinetics and the effect on polymerization. Biochem J. 2005;389(Pt 2):549-58.
626   42.   Chaudhuri AR, Khan IA, Luduena RF. Detection of disulfide bonds in bovine brain
627   tubulin and their role in protein folding and microtubule assembly in vitro: a novel disulfide
628   detection approach. Biochemistry. 2001;40(30):8834-41.
629   43.   Bibli SI, Hu J, Looso M, Weigert A, Ratiu C, Wittig J, et al. Mapping the Endothelial Cell
630   S-Sulfhydrome Highlights the Crucial Role of Integrin Sulfhydration in Vascular Function.
631   Circulation. 2021;143(9):935-48.
632   44.   Fu L, Liu K, He J, Tian C, Yu X, Yang J. Direct Proteomic Mapping of Cysteine
633   Persulfidation. Antioxid Redox Signal. 2020;33(15):1061-76.
634   45.   Farese S, Stauffer E, Kalicki R, Hildebrandt T, Frey BM, Frey FJ, et al. Sodium
635   thiosulfate pharmacokinetics in hemodialysis patients and healthy volunteers. Clin J Am Soc
636   Nephrol. 2011;6(6):1447-55.
637   46.   Brucculeri M, Cheigh J, Bauer G, Serur D. Long-term intravenous sodium thiosulfate in
638   the treatment of a patient with calciphylaxis. Semin Dial. 2005;18(5):431-4.
639   47.   Schlieper G, Brandenburg V, Ketteler M, Floege J. Sodium thiosulfate in the treatment
640   of calcific uremic arteriolopathy. Nat Rev Nephrol. 2009;5(9):539-43.
641
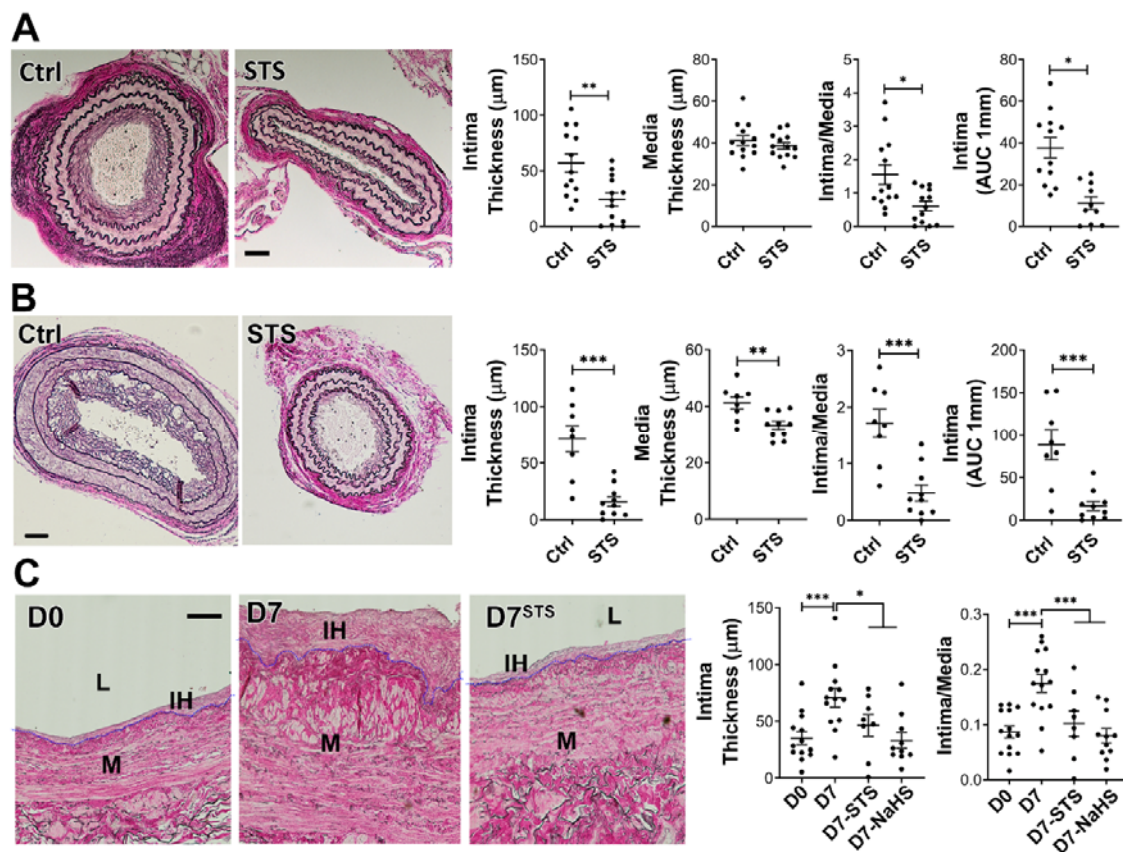642
643
644

645 **Figures and Figure legends**

646

647 **Figure 1. STS and NaHS decrease IH formation after carotid artery stenosis in mice**
648 **and in cultured human saphenous veins.**

649 **A-B**) WT (**A**) or LDLR^{-/-} mice (**B**) treated or not (ctrl) with 4g/L STS were subjected to the carotid
650 artery stenosis surgery. VGEL staining of left carotid cross sections and morphometric
651 measurements of intima thickness, media thickness, intima over media ratio and intima
652 thickness AUC. Scale bar 40μM. Data are mean±SEM of 13 (**A**) and 8 (**B**) animals per group.
653 *p<.05, **p<.01, ***p<.001 as determined by bilateral unpaired t-test. **C**) Intima thickness,
654 media thickness and intima over media ratio of freshly isolated human vein segments (D0) or
655 after 7 days (D7) in static culture with STS (15mM) or NaHS (100μM). Scale bar 60μm. Data
656 are mean±SEM of 12 different veins/patients. *p<0.05, **p<.01, ***p<.001, as determined by
657 repeated measures one-way ANOVA with Dunnett's multiple comparisons.
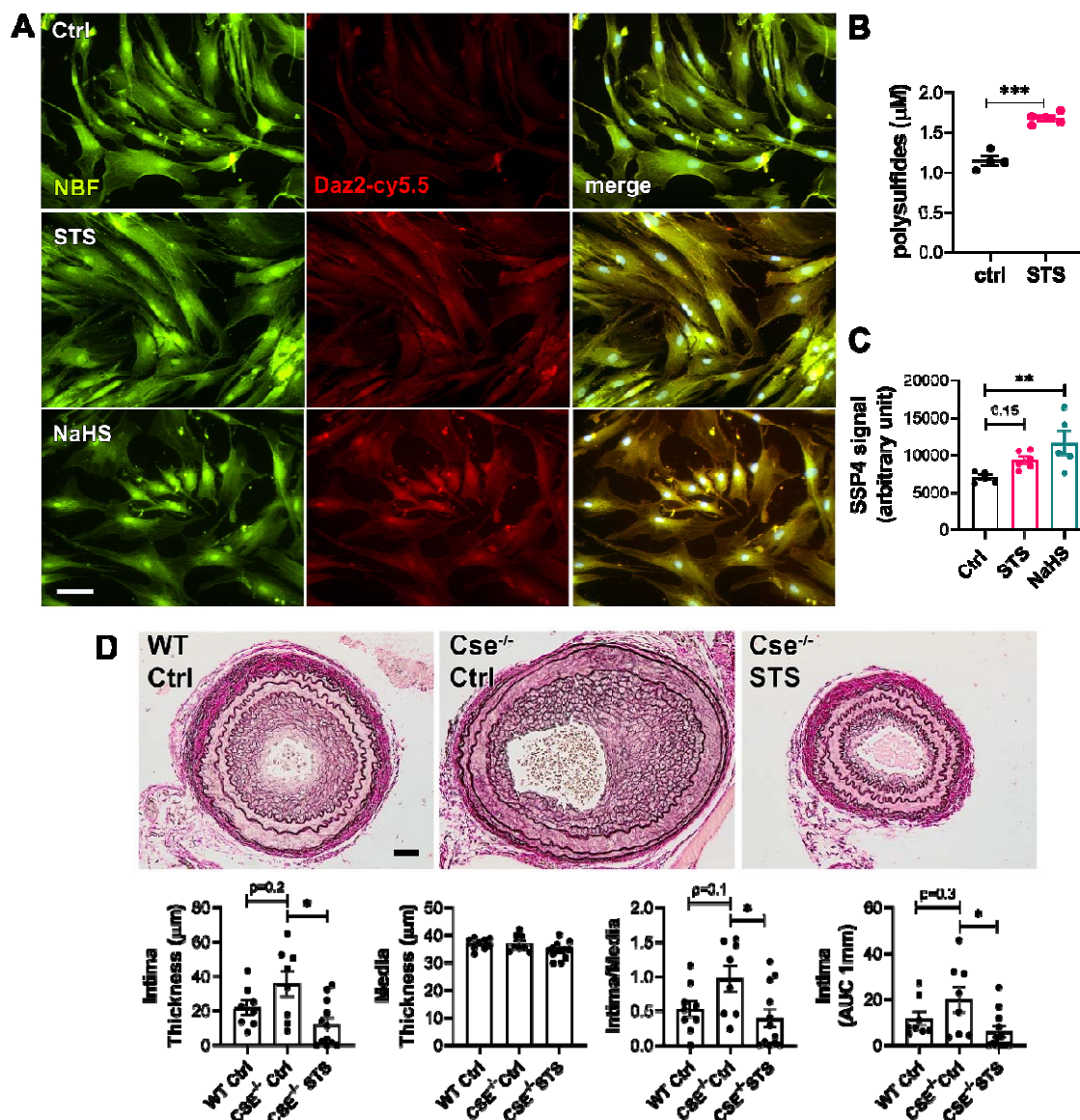
658

Figure 2. STS increases protein persulfidation.

A) In situ labeling of intracellular protein persulfidation assessed by DAz-2:Cy5.5 (red), normalized to NBF-adducts fluorescence (green), in VSMC exposed for 4 hours to NaHS (100 µM) or STS (15mM). Representative images of 5 independent experiments. Scale bar 20µm. **B)** Plasma polysulfides levels, as measured by the SSP4 probe, in mice treated 7 days with STS 4g/L. Data are scatter plots with mean ± SEM of 4 animals per group. ***p<.001 as determined by bilateral unpaired t-test. **C)** Polysulfides levels, as measured by the SSP4 probe in liver extracts of mice treated 7 days with STS 4g/L or NaHS 0.5g/L. Data are scatter plots with mean ± SEM of 5 animals per group. **p<.01 as determined by One-way ANOVA with post-hoc t-tests with Tukey's correction for multiple comparisons. **D)** Intima thickness, media thickness, intima over media ratio and intima thickness AUC of CAS operated mice measured 28 days after surgery in WT mice versus Cse^{-/-} mice treated or not (Cse^{-/-} Ctrl) with 4g/L STS (Cse^{-/-} STS). Scale bar 50µM. Data are scatter plots with mean ± SEM of 8 to 10 animals per group. *p<.05, **p<.01, as determined by one-way ANOVA with post-hoc t-tests with Tukey's correction for multiple comparisons.

676
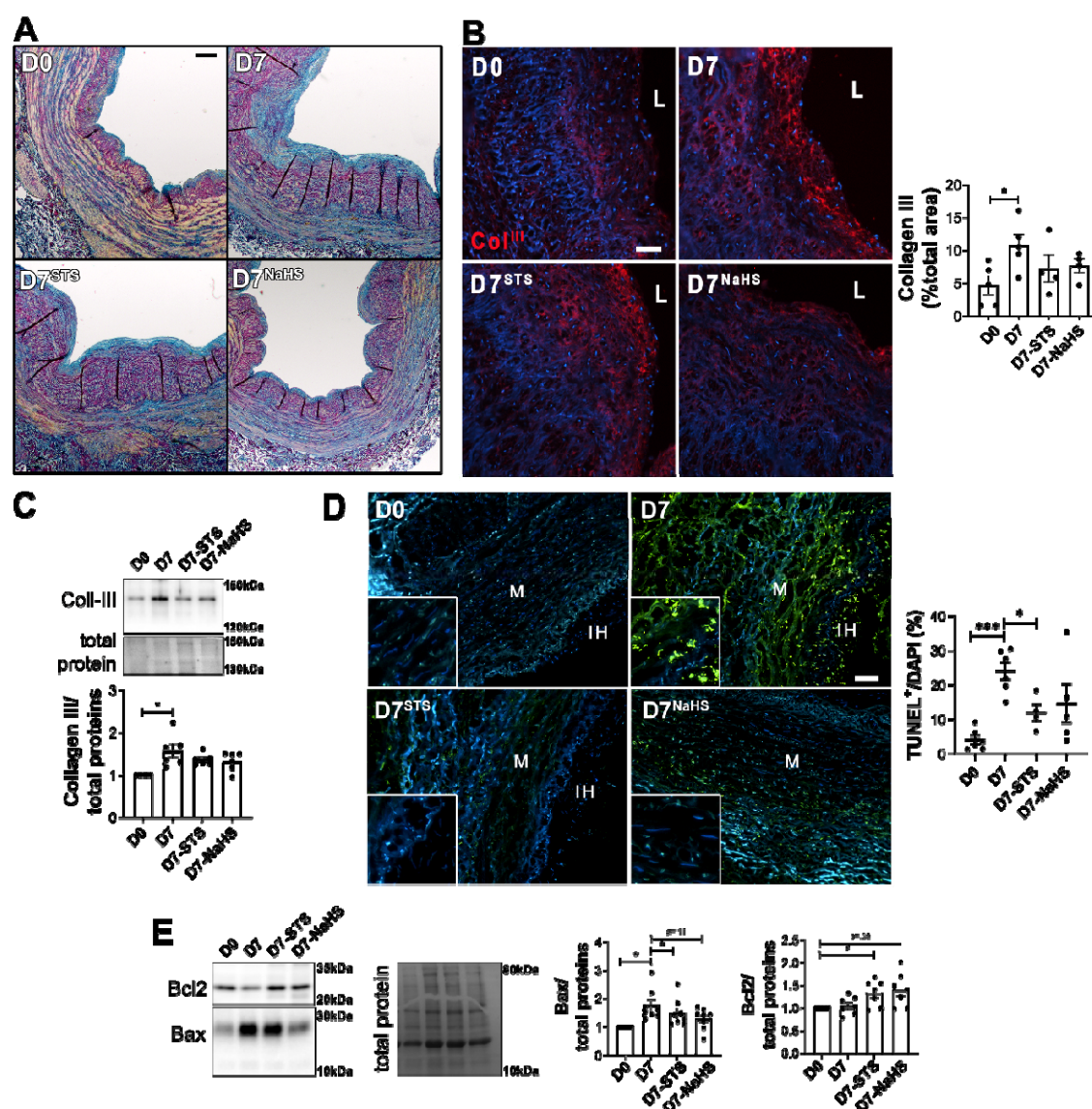
677

678 **Figure 3. STS decreases apoptosis and matrix deposition in human vein segments.**

679 Human vein segment at D0 or after 7 days of static culture with or without (D7) 15mM STS or
680 100μM NaHS. **A**) Representative Herovici staining of 5 different human vein segments.
681 Mature collagen I is stained pink; new collagen III is stained blue; cytoplasm is
682 counterstained yellow; nuclei are stained blue to black. Scale bar=80μm **B**) *Left panels:*
683 Representative collagen III immunofluorescent staining. Scale bar=50μm. *Right panel*
684 Quantitative assessment of Collagen III immunofluorescent staining. Data are scatter plots of
685 5 different veins with mean±SEM. *p<0.05 as determined by paired repeated measures one-
686 way ANOVA with Dunnett's multiple comparisons. **C)** Representative western blot of collagen
687 III over total protein and quantitative assessment of 6 different human vein segments. Data
688 are scatter plots with mean±SEM. *p<0.05 as determined by paired repeated measures one-
689 way ANOVA with Dunnett's multiple comparisons. **D)** *Left panels:* Representative TUNEL
690 staining in human vein segments. *Right panel:* Apoptosis is expressed as TUNEL positive
691 (green) over DAPI positive nuclei. Scale bar= 50μm**.** Data are scatter plots of 5 to 6 different
692 veins with mean±SEM. *p<.05, ***p<.001 as determined by mixed model analysis with
693 Dunnett's multiple comparisons. **E)** Representative western blot of Bax and Bcl2 over total

694 protein and quantitative assessment of 7 different human veins. Data are scatter plots with
695 mean±SEM. *p<0.05 as determined by repeated measures one-way ANOVA with Dunnett's
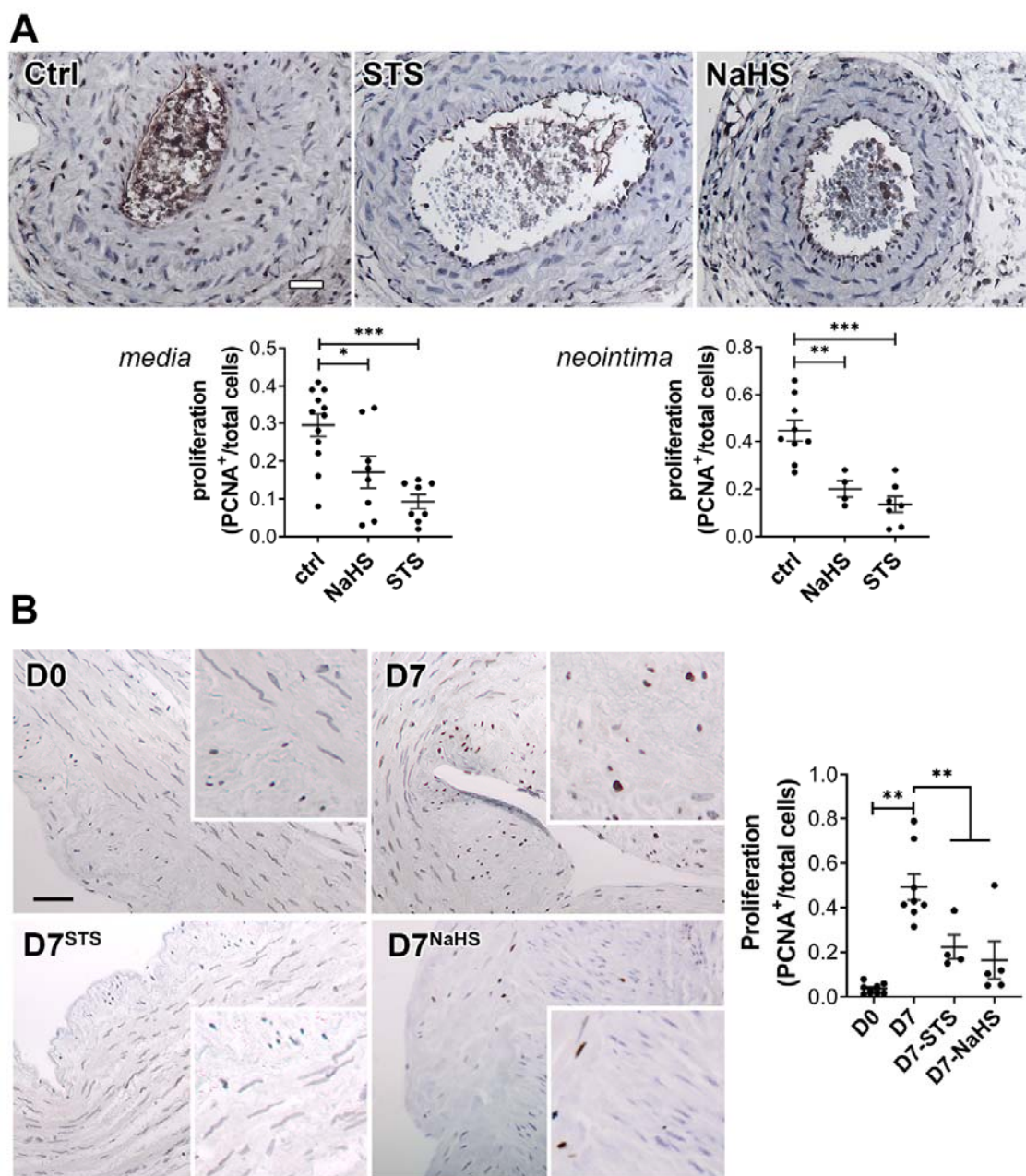696 multiple comparisons.

697

698

Figure 4. STS inhibits cell proliferation *in vivo* in mouse carotids and *ex-vivo* in human vein segments

699
700

701 PCNA immunostaining on CAS operated carotids in WT mice (**A**) treated or not (Ctrl) with
702 STS 4g/L or NaHS 0.5g/L for 28 days, and human vein segments (**B**) incubated or not (Ctrl)
703 with 15mM STS or 100μM NaHS for 7 days. Proliferation is expressed as the ratio of PCNA
704 positive (brown) nuclei over total number of nuclei. Data are scatter plots with mean±SEM.
705 (**A**) Scale bar 20μm. *p<.05, **p<.01, ***p<.001 as determined from 8 to 12 animals per
706 group by one-way ANOVA with Dunnett's multiple comparisons. (**B**) Scale bar 50μm **p<.01,

707   as determined from 5 to 7 different veins by mixed model analysis and Dunnett's multiple
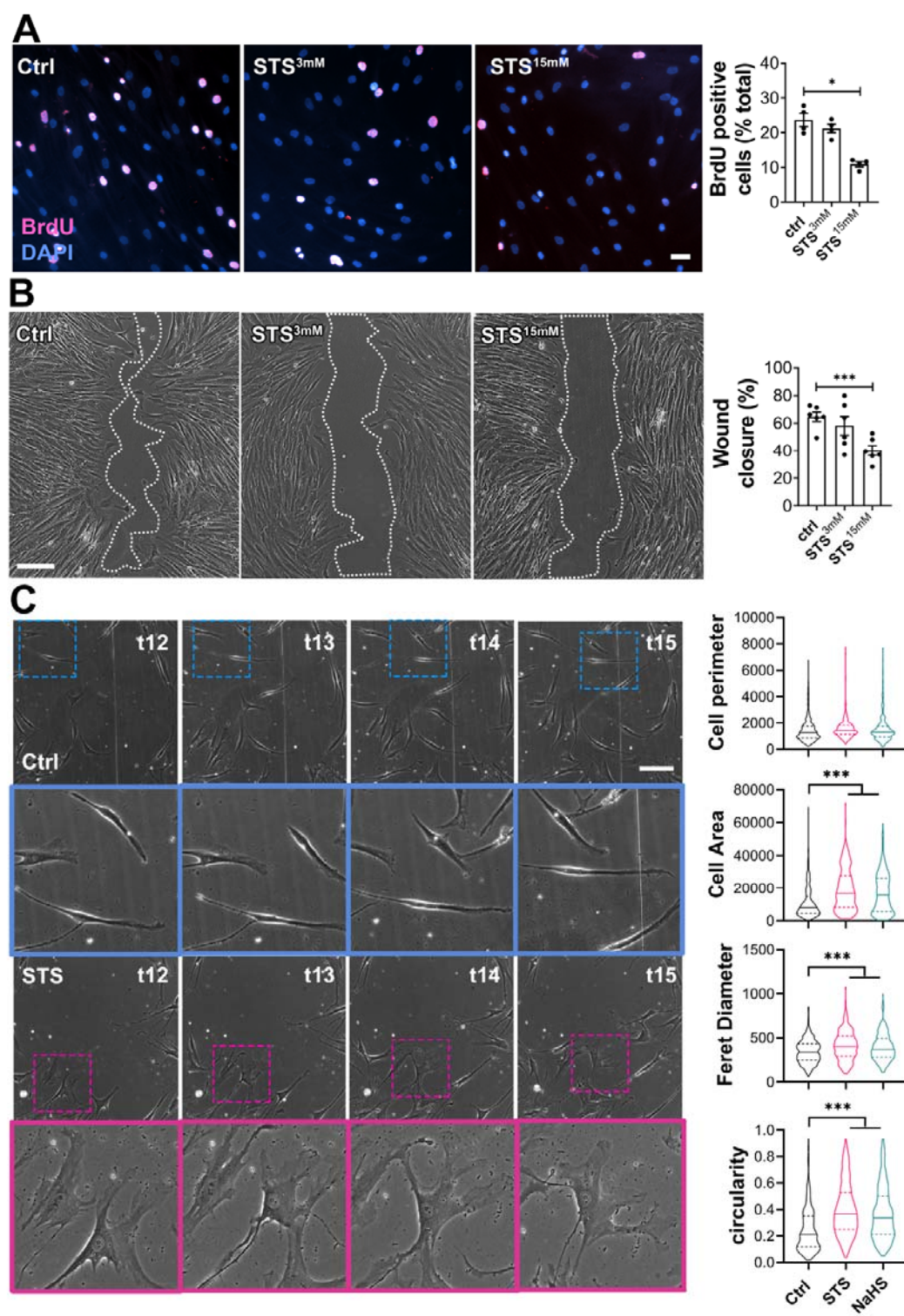708   comparisons.

709

710

711
712   **Figure 5. STS inhibits VSMC proliferation and migration *in vitro***

713 **A**) VSMC proliferation (BrdU incorporation) in cells treated or not for 24 hours with or without
714 (Ctrl) 3 or 15mM STS. Data are % of BrdU positive nuclei (pink) over DAPI positive nuclei.
715 Scale bar: 25μm. Data shown as mean±SEM of 6 different experiments. *p<.05 as
716 determined by repeated measures one-way ANOVA with Dunnett's multiple comparisons
717 tests. **B)** VSMC migration in cells treated or not for 24 hours with or without (Ctrl) 3 or 15mM
718 STS, as assessed by wound healing assay, expressed as the percentage of wound closure
719 after 10 hours. Scale bar: 100μm. Data are scatter plots with mean±SEM of 5 independent
720 experiments in duplicates. ***p<.001 as determined by repeated measures one-way ANOVA
721 with Dunnett's multiple comparisons. **C)** Bright field images of VSMC morphology in cells
722 exposed or not (Ctrl) to 15mM STS or 100μM NaHS, as measured as cell perimeter, cell
723 area, Feret diameter and circularity index assessed during wound healing assay. Data are
724 violin plots with median and quartiles (dotted lines) of 5 independent experiments. ***p<.001
725 as determined by one-way ANOVA with Dunnett's post-hot test. Scale bar: 80μm. Pink and
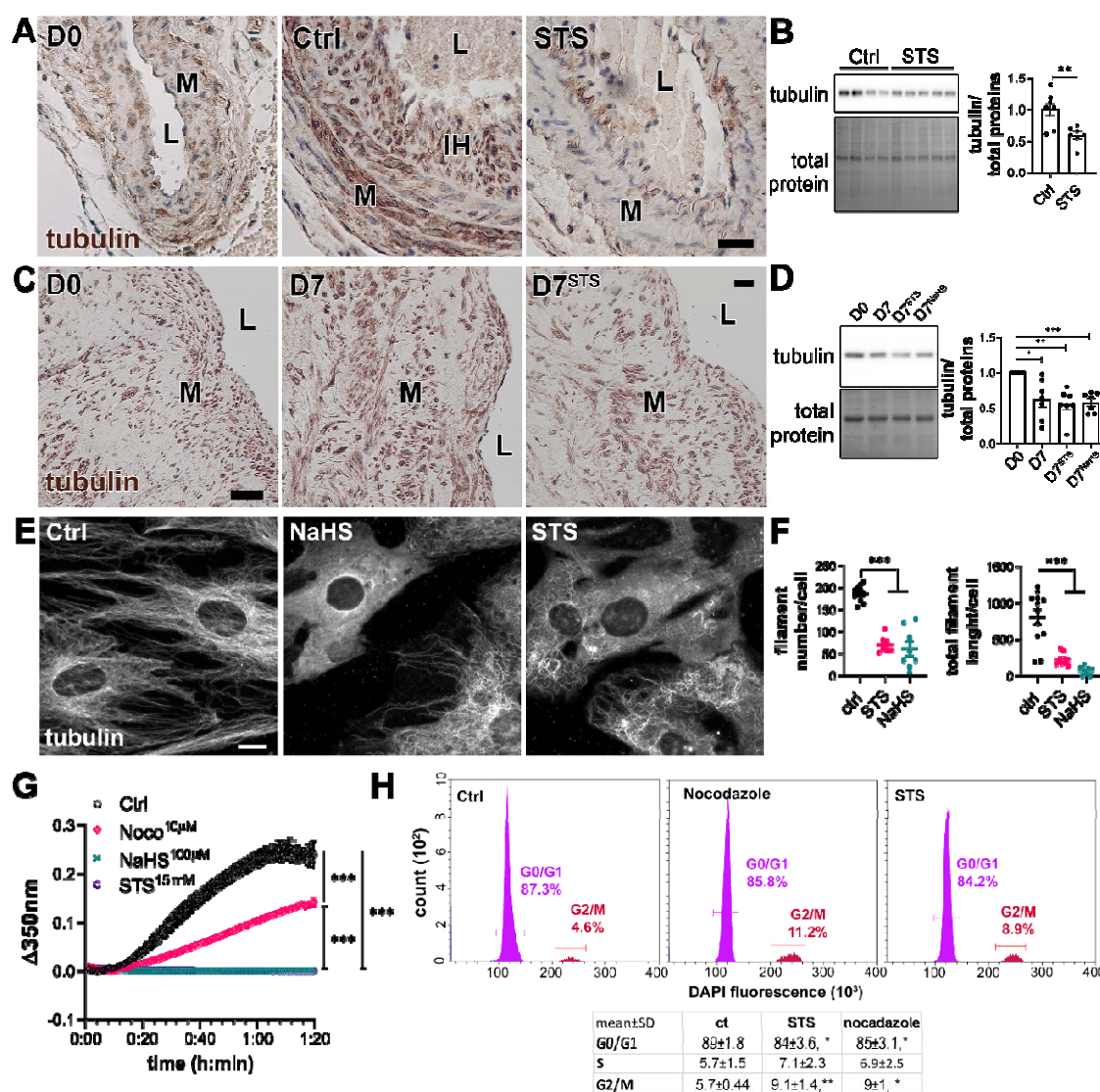726 blue insets are 3-fold magnifications of outlined areas.

727

728
729 **Figure 6. STS inhibits microtubule polymerization in VSMC**

730 **A)** α-tubulin immunolabelling in carotids of native (D0) or CAS-operated mice treated or not
731 (Ctrl) with STS 4g/L. L=Lumen; M= Media; IH= Intimal Hyperplasia. Images are

732 representative of 5 to 8 mice per group. **B)** WB analysis of α-tubulin over total protein in
733 aortas of mice treated or not (Ctrl) with STS 4g/L for 7 days. Data are scatter plots of 7 mice
734 per groups with mean±SEM with **p<.01, as determined by one-way ANOVA with Tukey's
735 multiple comparisons tests. **C)** α-tubulin immunolabelling in human vein segments kept or not
736 (D0) in culture in presence or not (Ctrl) of 15mM STS for 7 days. Scale bar 40μm. L=Lumen;
737 M= Media. Images are representative of 5 different veins. **D)** WB analysis of tubulin over total
738 protein in human vein segments kept or not (D0) in culture in presence or not (Ctrl) of 15mM
739 STS or 100 μM NaHS for 7 days. *p<.05, **p<.01, ***p<.001, as determined by repeated
740 measures one-way ANOVA from 7 different veins with Dunnett's multiple comparisons tests.
741 **E**) α-tubulin immunofluorescent staining in VSMC exposed or not to 15mM STS or 100 μM
742 NaHS for 8 hours. Images are representative of 5 independent experiments. Bar scale 10
743 μm. **F)** Quantitative assessment of microtubule filaments immunostaining per cell. Data are
744 representative of 3 independent experiments, 3 to 4 images per experiment per condition.
745 ***p<0.001 as determined by one-way ANOVA with Tukey's multiple comparisons tests. **G)**
746 *In vitro* tubulin polymerization assay in presence or not (Ctrl) of 15mM STS, 100μM NaHS or
747 10μM Nocodazole. Data are mean±SEM of 3 independent experiments. **H)** Flow cytometry
748 analysis of cell cycle (DNA content) using DAPI-stained VSMC treated or not (Ctrl) for 48
749 hours with 15mM STS or 10nM Nocodazole. *Upper panel*: representative histograms; *lower*
750 *panel*: table with mean±SD of 5 independent experiments. *p<0.05, **p<0.01 as determined
751 by one-way ANOVA with Dunnett's multiple comparisons tests.

752